Available online at www.sciencedirect.com

SciVerse ScienceDirect

Ceramics International 39 (2013) 4253–4262

CERAMICS INTERNATIONAL

www.elsevier.com/locate/ceramint

Preparation and characterization of Al_2O_3/TiC micro–nano-composite ceramic tool materials

Zengbin Yin[a,b], Chuanzhen Huang[a,b,*], Bin Zou[a,b], Hanlian Liu[a,b], Hongtao Zhu[a,b], Jun Wang[a,b]

[a]Centre for Advanced Jet Engineering Technologies (CaJET), School of Mechanical Engineering, Shandong University, Jinan 250061, PR China
[b]Key Laboratory of High-efficiency and Clean Mechanical Manufacture, Shandong University, Ministry of Education, PR China

Received 13 August 2012; received in revised form 6 October 2012; accepted 15 October 2012
Available online 16 November 2012

Abstract

An Al_2O_3-based composite ceramic tool material reinforced with micro-scale and nano-scale TiC particles was fabricated by a hot-pressing technology with cobalt additive in different sintering processes. The microstructure, indention cracks and phase composition of composites were characterized with scanning electron microscopy, transmission electron microscopy and X-ray diffraction. The experimental results showed that $Al_2O_3/TiC_\mu/TiC_n$ micro–nano-composite containing 6 vol% nano-scale TiC and 35 vol% micro-scale TiC, which were sintered under a pressure of 32 MPa at a temperature of 1650 °C in vacuum for 20 min, had optimum mechanical properties. The addition of both nano-scale TiC and Co contributed to the microstructure evolution and the improvement of mechanical properties. Effects of nano-scale TiC on mechanical properties were investigated. The toughening and strengthening mechanisms of micro–nano-composites were discussed.

Keywords: B. Composites; C. Mechanical properties; D. Al_2O_3; Strengthening and toughening mechanisms

1. Introduction

Al_2O_3-based ceramics exhibit excellent properties such as high thermal resistance, good chemical stability and wear resistance, which are required for materials used in modern cutting tools [1,2]. However, one of the inherent drawbacks of alumina is the relatively low fracture toughness. The brittleness and poor damage tolerance have limited the wide application of ceramics. During the past two decades, much effort has been made to improve the strength and toughness of ceramic materials. Several useful methods have been proposed, such as dispersion of different particles in a matrix [3], fiber or whisker reinforced composites [4] and phase transformation induced toughening as revealed by zirconia [5]. However, the strengthening effects of these secondary phases, like whiskers, short fibers and particles are limited.

The effect of nanoparticles on alumina matrix was first demonstrated by Niihara and Nakahira [6] who reported that the flexural strength and fracture toughness of monolithic alumina were increased from 350 MPa and 3 MPa $m^{1/2}$ to 1050 MPa and 4.7 MPa $m^{1/2}$ with 5 vol% SiC nanoparticles. Niihara proposed that strength was improved due to the refinement of microstructural scale which was from the order of the alumina grain size to the order of interparticles spacing, thus reducing the critical flaw size. Furthermore, strength increase can also be explained by the toughening effect caused by crack deflection due to the residual stress developed around SiC particles as a result of thermo-elastic mismatch with the alumina matrix. The concept of nano-composites, that involves the incorporation of some fine particles into the matrix, has been applied successfully in many ceramic systems which have already developed better mechanical properties [7–9]. Recently, grain size effects on mechanical properties of composite ceramics have been

*Corresponding author at: Centre for Advanced Jet Engineering Technologies (CaJET), School of Mechanical Engineering, Shandong University, Jinan 250061, PR China. Tel./fax: +86 531 88396913.
E-mail address: chuanzhenh@sdu.edu.cn (C. Huang).

0272-8842/$ - see front matter © 2012 Elsevier Ltd and Techna Group S.r.l. All rights reserved.
http://dx.doi.org/10.1016/j.ceramint.2012.10.277

widely studied [10–13]. The addition of multi-scale particles into the Al_2O_3-based ceramics has been found to be an effective method to enhance the flexural strength and fracture toughness [14–17].

The present work attempts to study the possibility of improving the mechanical properties by adding nano-scale TiC and micro-scale TiC together into the micro-scale Al_2O_3 matrix. The range of nano-scale TiC particles content was determined by calculating the ratio of fracture toughness of Al_2O_3 grain boundary (K_{cb}) to fracture toughness of Al_2O_3 grain (K_{cg}). The strengthening and toughening mechanisms were investigated together with the microstructure and phase composition.

2. Determination of nano-scale TiC content

With the additive nano-scale particles into micro-scale Al_2O_3 matrix, the nano-scale particles intend to enter into the Al_2O_3 grains forming intragranular structure [12,14–17]. The residual stress in the matrix generates due to the mismatch of thermal expansion coefficients between particles and matrix. It is reasonable that the residual stress accounts almost completely for the change of fracture mode in Al_2O_3-based composites by changing mechanical properties of the matrix and their interface, i.e., grain boundary toughness and grain toughness [18]. Kim et al. considered that the ratio of grain boundary toughness to the grain toughness K_{cb}/K_{cg} can dramatically influence the fracture mode of the ceramic materials, and the corresponding relation between K_{cb}/K_{cg} and percentage of transgranular fracture can be determined by 2D or 3D modeling, and when $K_{cb}/K_{cg} \in [0.75, 0.85]$, the optimum fracture toughness and strength of composite ceramics could be obtained [19]. This theory was proved to be effective by Zhang with considering the effect of residual stress on grain boundary toughness and grain toughness [20]. The change of grain boundary toughness ΔK_{cb} in the presence of residual stress can be given by the method proposed by Shi et al. [18] as follows:

$$\Delta k_{cb} = \frac{1}{\sqrt{\pi D}} \int_{-D}^{D} \sigma_m \left(\frac{D+x}{D-x} \right)^{1/2} dx = \sigma_m \sqrt{\pi D} \tag{1}$$

Where σ_m is the average residual stress in matrix which can be obtained by the model developed by Taya et al. [21], and D is the matrix grain size. The change of grain toughness ΔK_{cg}in the presence of σ_m can be calculated by the equation proposed by Taya et al. [21].

$$\Delta k_{cg} = 2\sigma_m \sqrt{\frac{2(\lambda - d)}{\pi}}, \lambda = 1.085 \frac{d}{\sqrt{f}} \tag{2}$$

where λ is the average inter-particle spacing, d is the mean particle size, f is the volume fraction of particles. Kim et al. [19] reported that the fracture toughness values of the alumina grain boundary and alumina single crystal were 1.16 MPa $m^{1/2}$ and 1.53 MPa $m^{1/2}$, respectively. As the residual compressive stress distributed in Al_2O_3 has effects to enhance the fracture toughness, so the K_{cb}/K_{cg} of Al_2O_3–TiC composites can be given on the basis of Eqs. (1) and (2).

$$\frac{K_{cb}}{K_{cg}} = \frac{1.16 + \Delta K_{cb}}{1.53 + \Delta K_{cg}} \tag{3}$$

considering that when sintering the particles size will grow about three to six times than that of original ones [22]. Taking D as 2 μm (original size 0.5 μm) and d as 160 nm (original size 40 nm), and the sintering temperature is 1650 °C. According to Eqs. (1)–(3), the K_{cb}/K_{cg} of Al_2O_3–TiC composites depending on nano-scale TiC volume content f can be obtained as shown in Fig. 1. According to Fig. 1 the content of nano-scale TiC in present work was selected as 3%, 6% and 9% in volume.

3. Experimental procedures

3.1. Materials preparation

The starting materials were α-Al_2O_3 powders with an average particle size of approximately 0.5 μm (purity: 99.99%, Zibo, China), nano-scale TiC with an average particle size of approximately 40 nm (purity: 99.9%, Shanghai, China) and micro-scale TiC with an average particle size of 0.5 μm (purity: 99%, Hefei, China). Co was used as sintering additive to promote the densification of the composite. Three different composition ratios were tested for the composites as shown in Table 1. The nano-scale TiC powders were prepared into suspensions using alcohol as the dispersing medium, and the dispersant PEG (polyethylene glycol, Shanghai, China) was added after ultrasonic dispersion (with SB5200 ultrasonic instrument

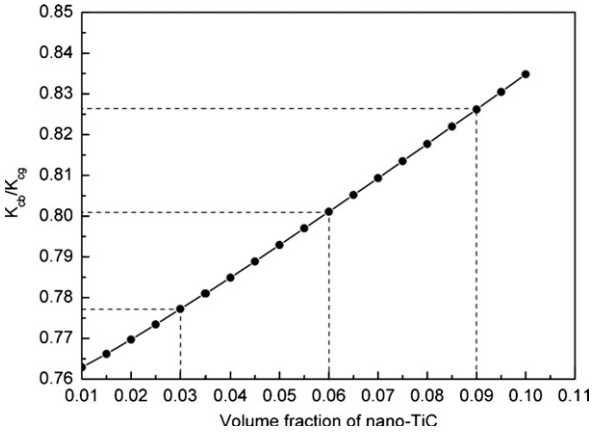

Fig. 1. K_{cb}/K_{cg} vs. volume fraction of nano-TiC.

Table 1
Composition (vol%) of different composites.

Composites	Al_2O_3(0.5 μm)	TiC(40 nm)	TiC(0.5 μm)	Co
ATT3	59	3	35	3
ATT6	56	6	35	3
ATT9	53	9	35	3

and D-7401-III motor stirrer, China) for 10 min. The suspensions were dispersed ultrasonically for 20 min after a pH of 9.0 (with PHS-25 digimatic pH-meter, China) was attained by the addition of $NH_3 \cdot H_2O$. After the nano-scale TiC particles suspension was dispersed well, they were then mixed with micro Al_2O_3, micro TiC and cobalt. The mixed slurries were ball-milled for 48 h, and then dried in a vacuum dry-type evaporator (Moder ZK-82 A, China). After drying, the ball-milled powders were sieved through a 200-mech sieve for further use. The dried powder was hot-pressed with an applied pressure of 32 MPa at a temperature of 1600–1700 °C with the holding time of 10–30 min in vacuum in a graphite die. The minor contamination caused by PEG was negligible.

3.2. Characterization

Sintered compacts were cut, ground and polished into specimens with a dimension of 3 mm × 4 mm × 35 mm. The flexural strength was measured using a three-point bending test (Model WD-10, China) with a span of 20 mm and loading velocity of 0.5 mm/min. The Vickers hardness was measured on the polished surface using a Vickers diamond pyramid indenter (Model 120, China) with a load of 196 N and a loading holding time of 15 s. The fracture toughness measurement of materials was determined by the Vickers indentation method proposed by Evans and Charles [23]. The fracture surfaces and cracks on the polished surfaces were observed by scanning electron microscopy (SEM, SUPRA-55, ZEISS, Germany). Phase identification was carried out by X-ray diffraction analysis (XRD, RAX-10A-X, Hitachi, Japan) with copper Kα radiation. Characterization of the microstructure, especially the distribution of secondary phase particles, dislocations was performed by transmission electron microscopy (TEM, JEM-2100, Japan). Thin foils of samples were prepared by grinding, dimpling and subsequent iron-beam thinning. The relative density of each specimen was measured by the Archimedes' method with distilled water as the medium and 3 specimens were tested for each experimental condition.

4. Results and discussion

4.1. Mechanical properties and microstructure

4.1.1. Effect of nano-TiC and sintering time on mechanical properties and microstructure

Effects of the content of nano-scale TiC and sintering time on mechanical properties of composites sintered at 1650 °C are shown in Fig. 2(a)–(c). It can be seen that the composite containing 6 vol% of nano-scale TiC have optimal comprehensive mechanical properties. SEM micrographs of

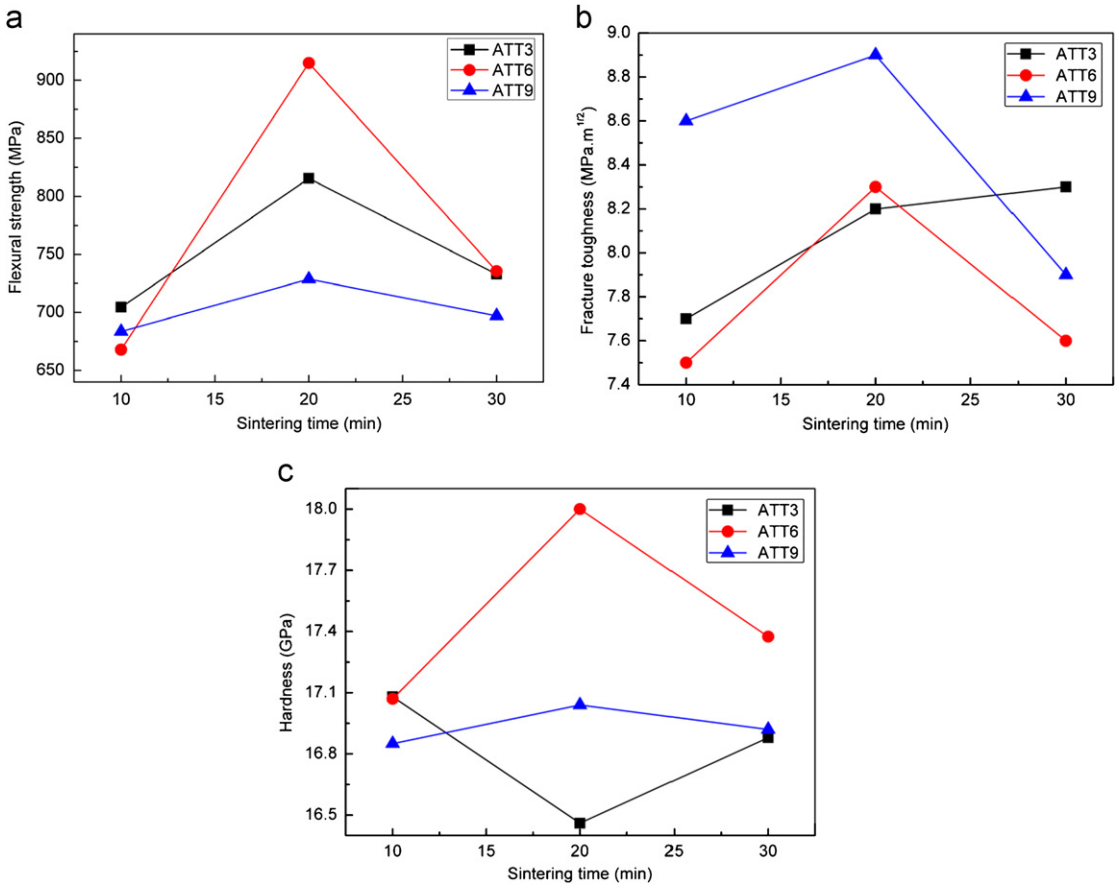

Fig. 2. Effect of content of nano-scale TiC and sintering time on (a) flexural strength, (b) fracture toughness and (c) hardness of composites sintered at 1650 °C.

the fracture surface of micro–nano-composites containing 3, 6 and 9 vol% of nano-scale TiC, which were sintered under a pressure of 32 MPa at the temperature of 1650 °C for 20 min, are shown in Fig. 3. It can be seen that the fracture surfaces of the three different composites were characterized by a mixed mode of intergranular and transgranular fracture. For composite ATT3 with lower content of nano-scale TiC, the grain size distribution is not homogeneous with abnormal grain growth as shown in Fig. 3(a). It is because that lower content of TiC cannot distribute in the interspaces of large particles uniformly and prohibit micro-Al_2O_3 grains growth effectively in the course of sintering. With an increase in the content of nano-scale TiC, the grain size becomes fine and homogeneous as shown in Fig. 3(b), which is attributed to that nano-scale TiC particles located at grain boundaries can prevent Al_2O_3 grain boundaries from moving by pinning boundaries and prohibit the growth of Al_2O_3 grains as shown in Fig. 4. Meanwhile, many nano-scale TiC particles may act as the nucleus inside the Al_2O_3 grains for the formation of intragranular structures. Both intergranular and intragranular TiC particles contributed to the well dense structure and small grain size, which are beneficial for the high comprehensive mechanical properties of composite ATT6. However, when the content of nano-scale TiC increases further, the excessive amount of nano-scale TiC particles tend to aggregate together, resulting in partial agglomerations as shown in Fig. 3(c). As the large specific surface area and high activity of nano-particles, the agglomerate particles grow fast and develop into large grains. The interspaces distributed among particles cannot be eliminated timely and mass of pores were entrapped into the grown grains due to the fast moving grain boundaries. This results in poor densification and is harmful to flexural strength and hardness. Therefore, for the flexural strength of composites, the nano-scale particles have an optimum content. When the content of nano-scale particles is lower than optimum content, the grain boundaries are not "toughened" enough, so the highest strength cannot be obtained. Larger than its optimum content, the grains are "embrittled", so the fracture is mainly transgranular, and the strength begins to decrease [20]. The fracture toughness of ATT9 is better

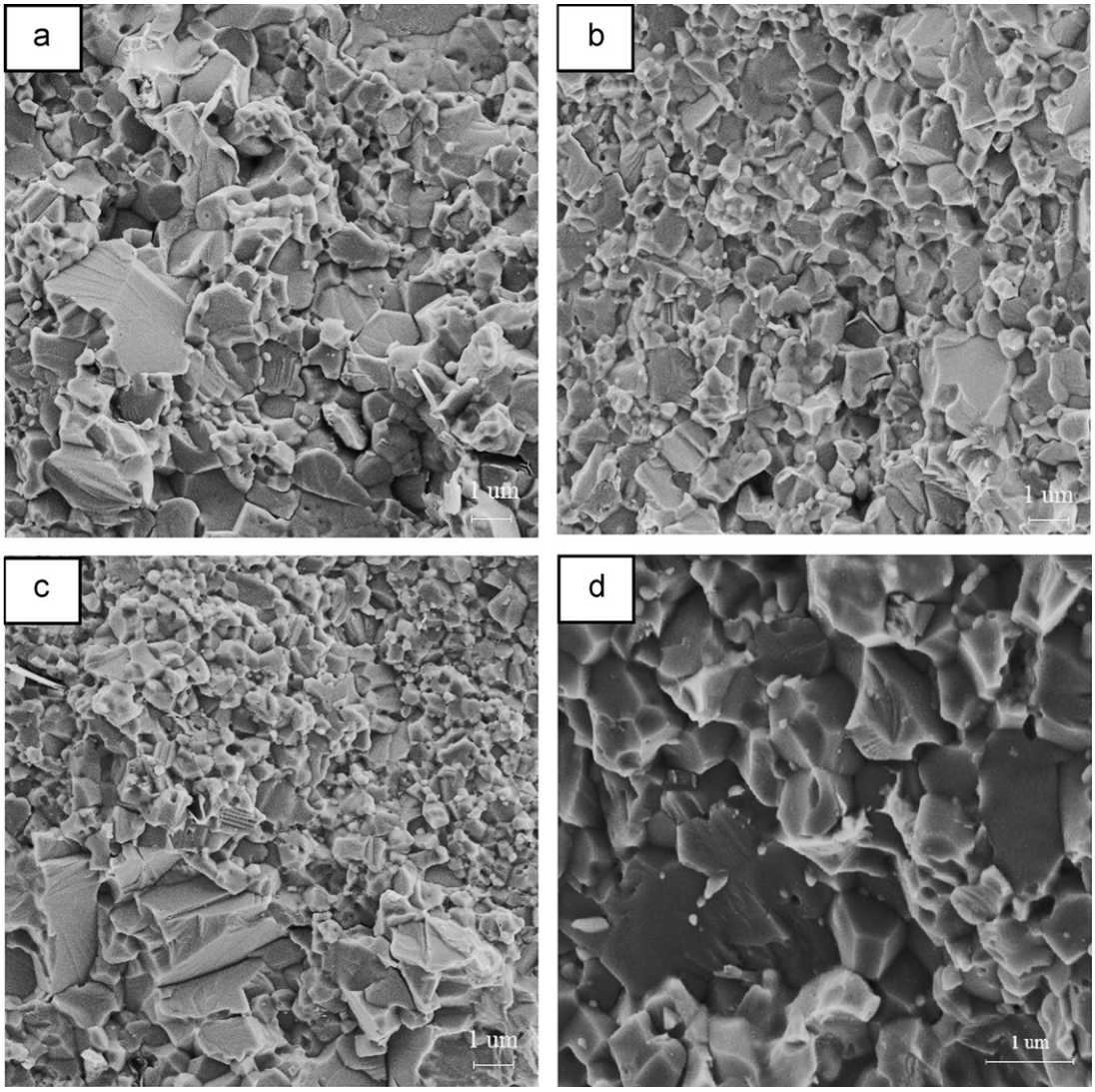

Fig. 3. SEM micrographs of fracture surface of micro–nano-composites containing (a) 3, (b) and (d) 6 and (c) 9 vol% nano-scale TiC.

than those of the other two may be due to the sectional large grains, which was proved that large grains contribute much to toughness and small grains have little toughening effect [13]. Additionally, the actual average grain size of D and d is 1.6 μm and 145 nm (observed in SEM and TEM micrographs shown in Fig. 3(d), Fig. 4 and Fig. 9), respectively. With Eqs. (1)–(3) when $K_{cb}/K_{cg} \in [0.75, 0.85]$, the volume fraction of nano-TiC is about between 1% and

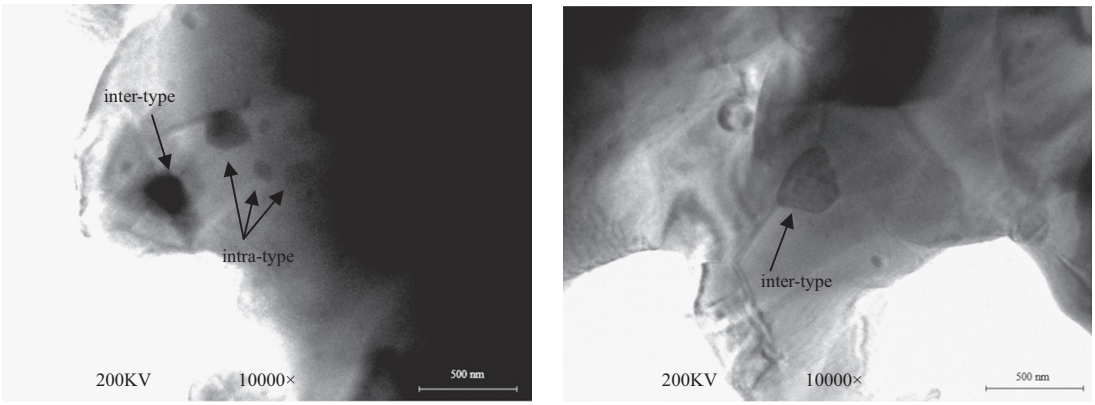

Fig. 4. TEM micrograph of composite ATT6.

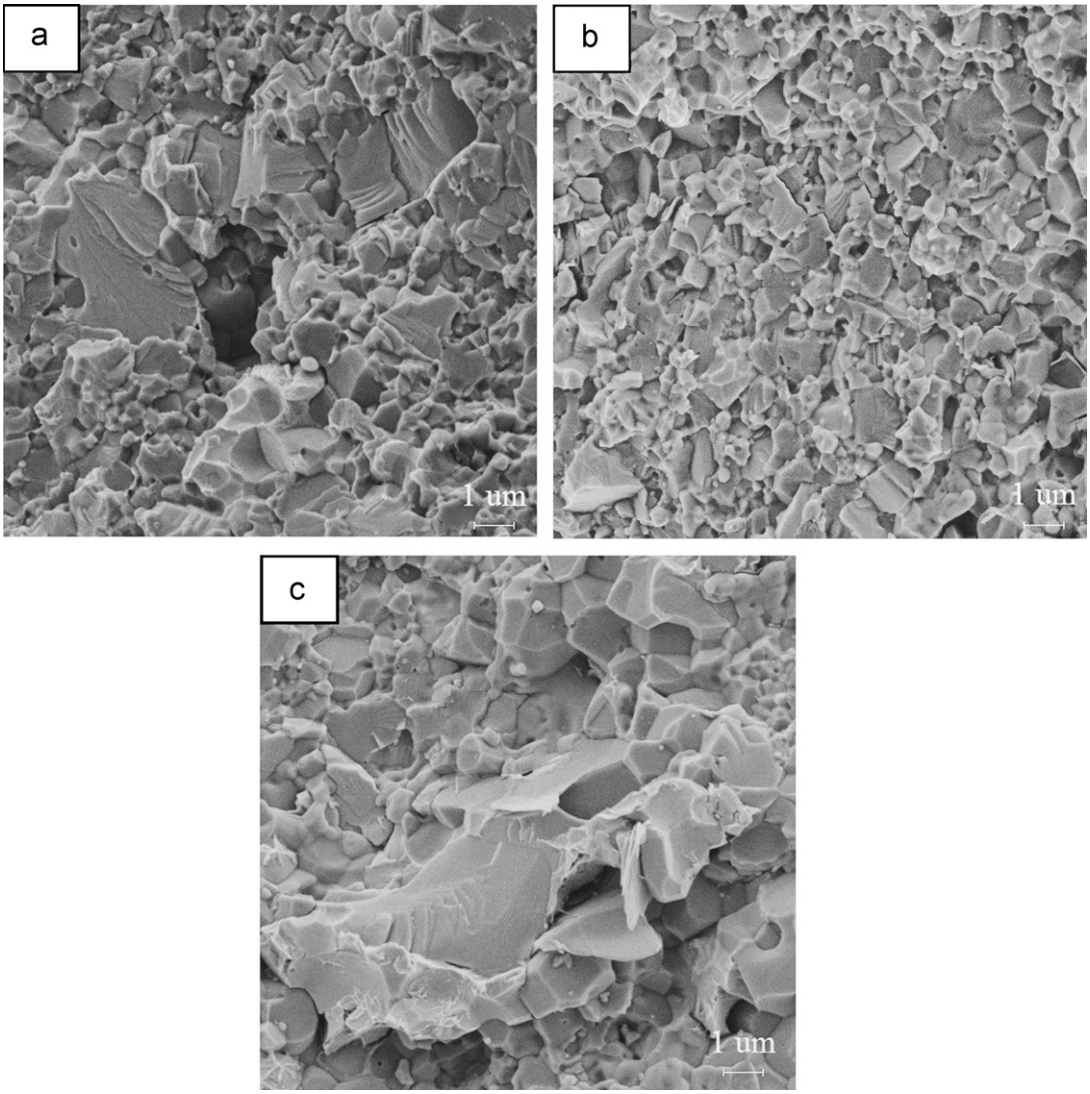

Fig. 5. SEM micrographs of fracture surfaces of ATT6 composites sintered under 32 MPa at 1650 °C for (a) 10 min, (b) 20 min and (c) 30 min.

13.3%, and the content of nano-TiC in present research is among this range. It demonstrates that it is feasible to calculate K_{cb}/K_{cg} by using the assumed D (2 μm) and d (160 nm) in the present micro–nano-composite.

When the sintering time is less than 20 min, the flexural strength, hardness and toughness of ATT6 composite increase with the sintering time as shown in Fig. 2(a)–(c). However, the mechanical properties decrease dramatically as sintering time increase further. SEM micrographs of fracture surfaces of ATT6 composite sintered under 32 MPa at 1650 °C for 10, 20 and 30 min are shown in Fig. 5(a)–(c).

When the sintering time is 10 min, the densification of the composite is poor, leaving numbers of pores at boundaries as shown in Fig. 5(a). The residual pores can cause stress concentration and weaken grain boundaries, which impairs mechanical properties of composites. As the sintering time increases up to 30 min, good densification can be obtained, but the abnormal grain growth appears which is detrimental to the flexural strength according to Hall–Petch relationship.

4.1.2. Effect of sintering temperature on the mechanical properties and microstructure

The effect of sintering temperature on mechanical properties of micro–nano-composites sintered under 32 MPa at 1600, 1650 and 1700 °C for 20 min are shown in Fig. 6. The XRD patterns of composite ATT6 sintered at different temperature are shown in Fig. 7. It can be seen that no chemical reaction occurred between Al_2O_3, TiC and Co from 1600 °C to 1700 °C, indicating the excellent chemical compatibility among them.

It can be seen from Fig. 6 that flexural strength and fracture toughness increase as the sintering temperature increases from 1600 to 1650 °C, but the flexural strength decreases drastically with the further increase of

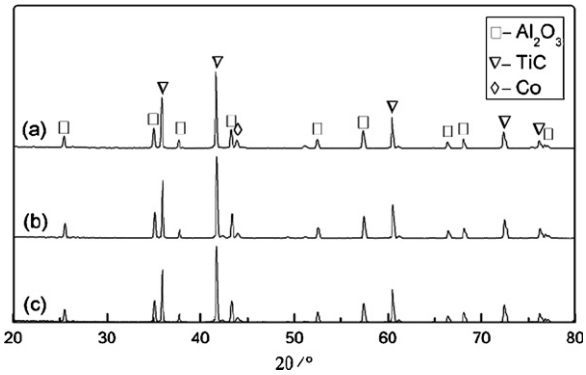

Fig. 7. XRD patterns of ATT6 sintered at different temperatures under 32 MPa for 20 min, (a) 1600 °C, (b) 1650 °C and (c) 1700 °C.

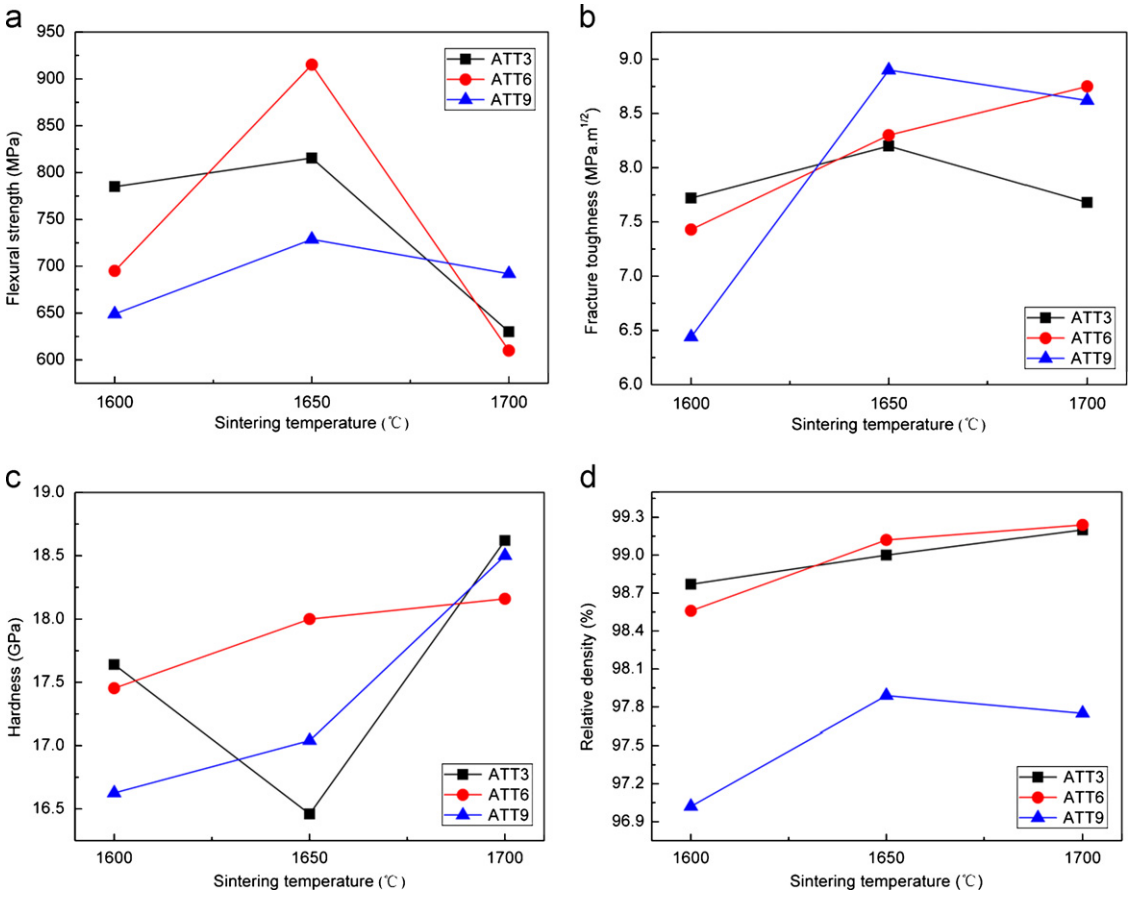

Fig. 6. Effect of sintering temperature on (a) flexural strength, (b) fracture toughness, (c) hardness of composites and (d) relative density sintered under 32 MPa for 20 min.

temperature, on the other hand the fracture toughness decreases slightly as temperature increases. However, the hardness of the composites increases gradually. This is because that composites become dense and pores will be closed gradually with an increase in sintering temperature as shown in Fig. 6(d). It can be seen from Fig. 8(a) when the sintering temperature is 1600 °C there are lots of pores distributed not only at grain boundaries but also in grains. The porosity is an important factor that influences the strength of composites. Pores not only decrease the loading cross-sectional area but also lead to stress concentration, so they decrease the strength of composites [11]. With the sintering temperature increases to 1700 °C the fracture surface is rough and there are little cleavage steps as shown in Fig. 8(c), which means the fracture mode is mainly intergranular fracture. And the high sintering temperature will make the movement of grain boundaries fast, leading to the excessive grain growth [24] which is harmful to flexural strength but beneficial for fracture toughness to some extent [13].

5. Strengthening and toughening mechanisms

Compared to Fig. 3, the fracture mode of micro–nano-composites is a mixture of transgranular and intergranular types, presenting a more complicated fracture mode, which leads to the improved mechanical properties. A fraction of nano-scale TiC particles distribute at grain boundaries as shown in Fig. 4. The reason for the intragranular fracture mode may be the pinning effect of TiC particles distributed at grain boundaries, which interlocks the Al_2O_3 grain boundaries and subsequently impede the crack extension along interfaces. Meanwhile, TiC particles located at grain boundaries suppress the movement of boundaries during sintering, leading to reduced grain size and fine microstructure. According to Hall–Petch relationship the flexural strength increases as the grain size decreases. Moreover, the cobalt has great effects on improving mechanical properties. The cobalt distributed uniformly in the matrix and mostly located at interfaces between Al_2O_3 and TiC grains. The cobalt distributed at grain boundaries not only reduces the

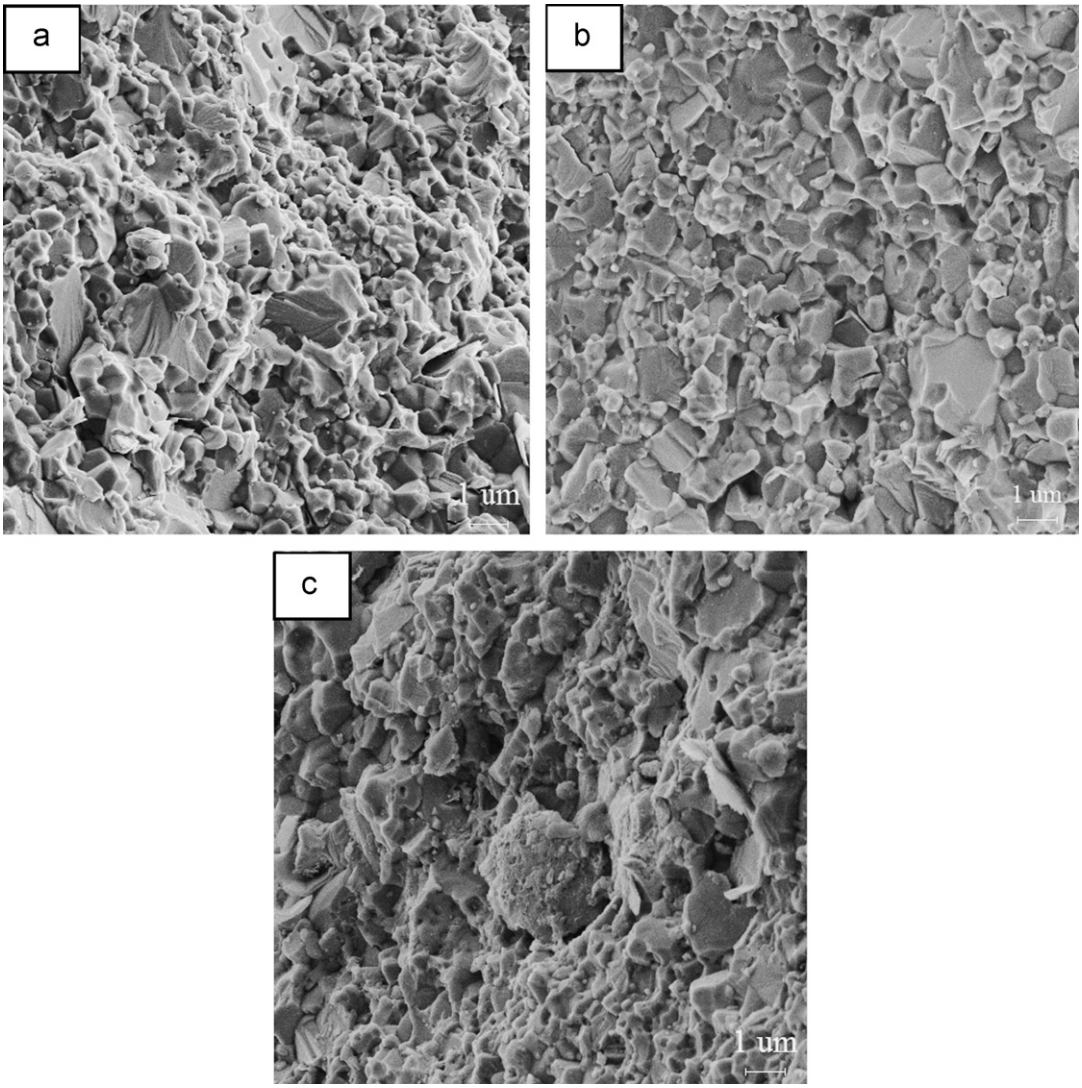

Fig. 8. SEM micrographs of fracture surfaces of ATT6 composites sintered under 32 MPa for 20 min, at (a) 1600 °C, (b) 1650 °C and (c) 1700 °C.

free energy of the grain boundary and restrains the grain boundary movement but also improves the interfacial bonding strength, thus leading to the homogeneous microstructure and the change of fracture mode [25]. Additionally, the melting point of cobalt is much lower than the sintering temperature. Cobalt becomes fluid and can fill pores among grains, thus the composite can possess a high relative density [26]. A regular array of hexagonal dislocations was observed in the Al_2O_3 grain around the intragranular nano-TiC particle as shown in Fig. 9 as a result of the thermal expansion mismatch inducing complex residual stress field, which could release the residual tensile stress existing in the matrix and improve the strength of composite.

The thermal expansion coefficients of Al_2O_3 and TiC are $8.4 \times 10^{-6}\,K^{-1}$, $7.4 \times 10^{-6}\,K^{-1}$, respectively. The thermal expansion mismatch between them would generate residual compressive stress on interfaces between Al_2O_3 and TiC which can enhance the interfacial bonding strength. However, the induced radial tensile stress in the matrix would weaken Al_2O_3 grains. When the propagating crack encounters hard particles, it would be deflected into the weakened matrix, where the crack would be impeded by the intragranular particles and deflected again as shown in region A of Figs. 10 and 11(a). The black phase is Al_2O_3, the gray phase is TiC and the white phase is Co. On account of the complex residual stress around TiC particles when the front of the crack encounters TiC particles, the crack tends to deflect and propagate mainly around TiC particles, occasionally passing through the hard TiC particles as indicated by narrows in Fig. 10, which is beneficial for improving the toughness by the increased consumption of fracture energy as a result of the residual compressive stress distributed both in interfaces and in TiC particles have effects to close cracks. Crack bridging is popular in present micro–nano-composite and plays an

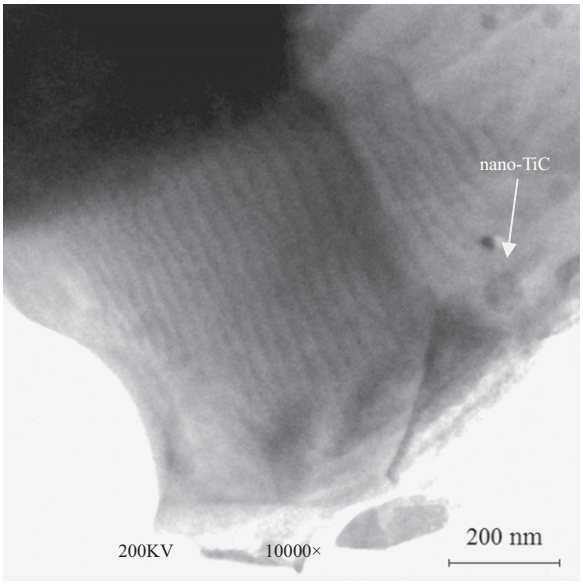

Fig. 9. TEM micrograph of composite ATT6.

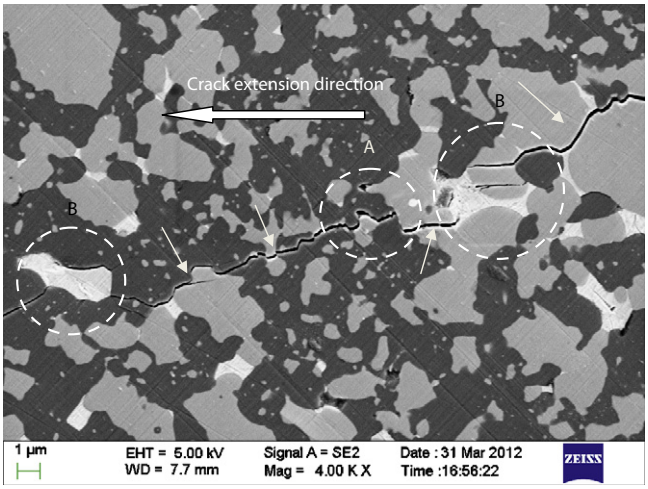

Fig. 10. Vicker's indentation crack extension paths of composite ATT6.

effective role in improving the fracture toughness. Crack bridging by the matrix, TiC particles and Co were observed in region B of Fig. 10 and Fig. 11(b). The crack bridging combinations connect two surfaces of a crack and provide with a force which makes two surfaces of a crack draw close. This results in the increase of stress strength factor with the extension of crack. The bridged crack can further extend only after making the bridging TiC particles to be stripped off the Al_2O_3 matrix or fractured as shown in Fig. 11(c). For the single bridge-rupture mechanism, the cumulative amount of surface-exposed crack length is approximately three times than that of the shortest-line path through the bridging sites [4]. So, during this process a great deal of fracture energy will be absorbed, crack extension energy will be expended, and the fracture toughness of the composites will be enhanced [11]. Therefore, higher value of fracture toughness and flexural strength should be attributed to the interaction of more effective energy consuming mechanisms in the micro–nano-composite.

6. Conclusions

(1) The range of nano-scale TiC particles content was determined by calculating the ratio of fracture toughness of Al_2O_3 grain boundary (K_{cb}) to fracture toughness of Al_2O_3 grain (K_{cg}) under the consideration of the influence of residual stress on K_{cg} and K_{cb}, which reduced the blindness of choosing the content of nano-particles and decreased experiment workload.

(2) The micro–nano-composite with optimum mechanical properties were sintered under a pressure of 32 MPa at 1650 °C for 20 min. The optimum mechanical properties was obtained as the content of nano-TiC particles was 6 vol%. The optimum mechanical properties are a flexural strength of 916 MPa, a fracture toughness of 8.3 MPa $m^{1/2}$ and a hardness of 18 GPa, which meet the requirements for cutting tool materials.

(3) Several strengthening and toughening mechanisms, such as grain refining, a mixed fracture modes of transgranular

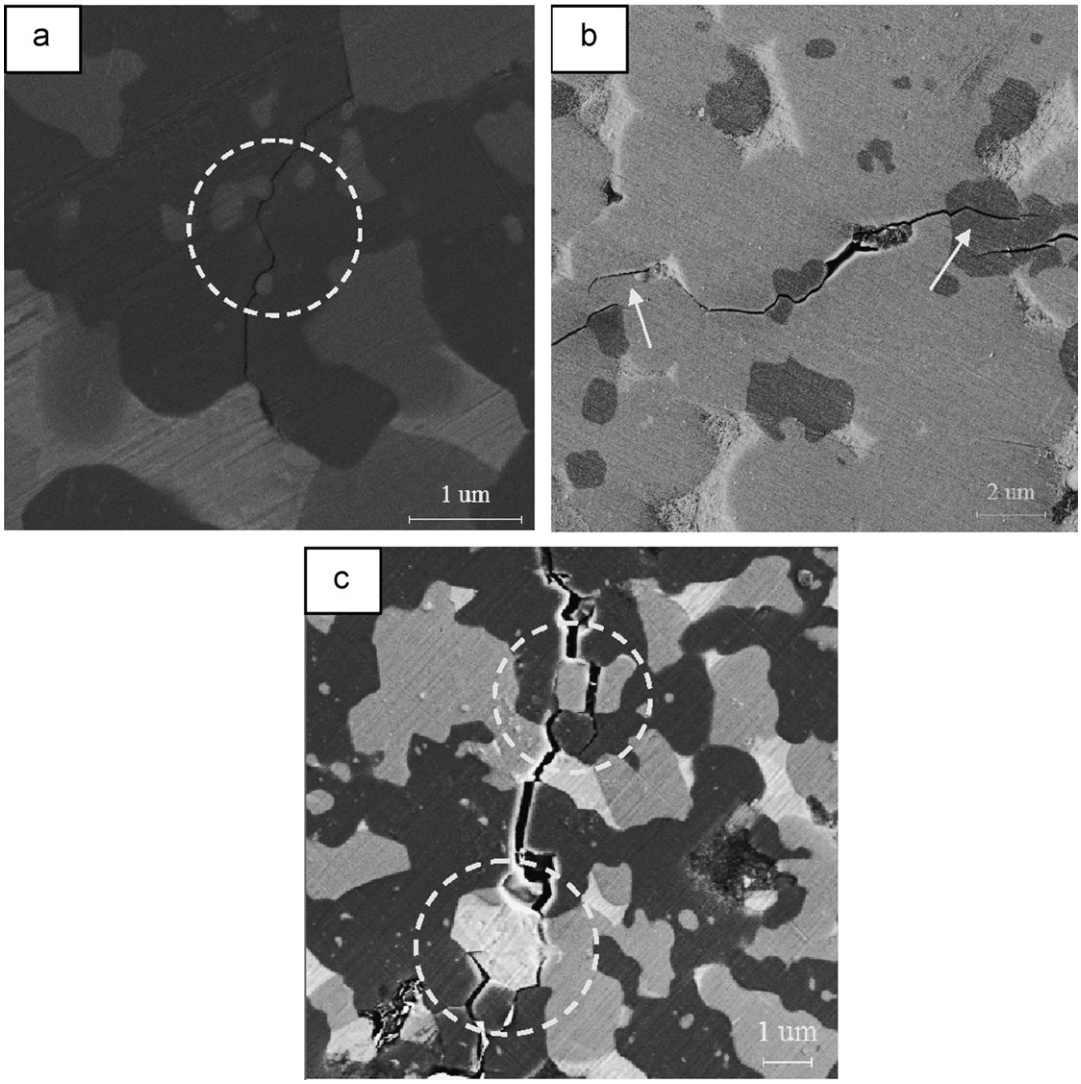

Fig. 11. Vicker's indentation crack extension paths of composite ATT6, (a) the second crack deflection, (b) crack bridging and (c) particles stripped off the matrix.

and intergranular, crack deflection, dislocation and crack bridged by matrix, particles and cobalt, acted simultaneously in ATT6 micro–nano-composite. These mechanisms could significantly improve the mechanical properties of the composite.

Acknowledgments

The work is supported by National Natural Science Foundation of China (50975161 and 51005136), and Key Special Project of Numerical Control Machine Tool (2012ZX04003-051).

References

[1] L. Carroll, M. Sternitzke, B. Derby, Silicon carbide particle size effects in alumina-based nanocomposites, Acta Materialia 44 (1996) 4543–4552.
[2] A.G. Evans, Perspective on the development of high-toughness ceramics, Journal of the American Ceramic Society 73 (1990) 187–206.
[3] W. Acchar, Y.B.F. Silva, C.A. Cairo, Mechanical properties of hot-pressed ZrO_2 reinforced with (W, Ti) C and Al_2O_3 additions, Materials Science and Engineering A 527 (2010) 480–484.
[4] B. Zou, C.Z. Huang, H.L. Liu, Study of the mechanical properties, toughening and strengthening mechanisms of Si_3N_4/Si_3N_{4w}/TiN nanocomposite ceramic tool materials, Acta Materialia 55 (2007) 4193–4202.
[5] Z. Zhao, L. Zhang, Y. Song, Microstructures and mechanical properties of Al_2O_3/ZrO_2 composite produced by combustion synthesis, Scripta Materialia 53 (2005) 995–1000.
[6] K. Niihara, A. Nakahira, Strengthening and toughening mechanisms in nanocomposite ceramics, Annales Des Chimie France 16 (1991) 479–486.
[7] N. Liu, Y.D. Xu, H. Li, Effect of nano-micro TiN addition on the microstructure and mechanical properties of TiC based cermets, Journal of the European Ceramic Society 22 (2002) 2409–2414.
[8] J. Zhao, X. Ai, Z. Lu, Preparation and characterization of Si_3N_4/TiC nanocomposite ceramics, Materials Letters 60 (2006) 2810–2813.
[9] Y. Yang, Y. Wang, W. Tian, Reinforcing and toughening alumina/titania ceramic composites with nano-dopants from nanostructured composite powders, Materials Science and Engineering A 508 (2009) 161–166.
[10] X.Y Teng, H.L. Liu, C.Z. Huang, Effect of Al_2O_3 particle size on the mechanical properties of alumina-based ceramics, Materials Science and Engineering A 452 (2007) 545–551.

[11] N. Liu, M. Shi, Y.D. Xu, Effect of starting powders size on the Al_2O_3–TiC composites, International Journal of Refractory Metals and Hard Materials 22 (2004) 265–269.
[12] M. Cao, S. Wang, W. Han, Influence of nano-sized SiC particle on the fracture toughness of ZrB_2-based nanocomposite ceramic, Materials Science and Engineering A 527 (2010) 2925–2928.
[13] J.H. Gong, H.Z. Miao, Z. Zhao, Effect of TiC particle size on the toughness characteristics of Al_2O_3–TiC composites, Materials Letters 49 (2001) 235–238.
[14] Y.L. Dong, F.M. Xu, X.L. Shi, Fabrication and mechanical properties of nano-/micro-sized Al_2O_3/SiC composites, Materials Science and Engineering A 504 (2009) 49–54.
[15] H. Reveron, O. Zaafrani, G. Fantozzi, Microstructure development, hardness, toughness and creep behaviour of pressureless sintered alumina/SiC micro-nanocomposites obtained by slip-casting, Journal of the European Ceramic Society 30 (2010) 1351–1357.
[16] C.H. Xu, Preparation and performance of an advanced multiphase composite ceramic material, Journal of the European Ceramic Society 25 (2005) 605–611.
[17] J. Zhao, X.L. Yuan, Y.H. Zhou, Processing and characterization of an Al_2O_3/WC/TiC micro-nano-composite ceramic tool material, Materials Science and Engineering A 527 (2010) 1844–1849.
[18] J.L. Shi, Z.L. Lu, J.K. Guo, Model analysis of boundary residual stress and its effect on toughness in thin boundary layered yttria-stabilized tetragonal zirconia polycrystalline ceramics, Journal of Materials Research 15 (2000) 727–732.
[19] B.N. Kim, S. Wakayama, M. Kawahara, Characterization of 2-dimensional crack propagation behavior by simulation and analysis, International Journal of Fracture 75 (1995) 247–259.
[20] F.C. Zhang, H.H. Luo, T.S. Wang, Stress state and fracture behavior of alumina–mullite intragranular particulate composites, Composites Science and Technology 68 (2008) 3245–3250.
[21] M. Taya, S. Hayashi, A.S. Kobayashi, Toughening of a particulate-reinforced ceramic-matrix composite by thermal residual stress, Journal of the American Ceramic Society 73 (1990) 1382–1391.
[22] Z.Z. Jin, The particles size effect on composite ceramic, Journal of the Chinese Ceramic Society 23 (1995) 610–616.
[23] A.G. Evans, E.A. Charles, Fracture toughness determinations by indentation, Journal of the American Ceramic Society 59 (1976) 371–372.
[24] J.F. Tong, D.M. Chen, Y.H. Chen, The effect of hot pressing parameters on mechanical properties of nano-SiC–Al_2O_3/TiC, Powder Metallurgy Technology 18 (2000) 102–105.
[25] J. Li, J.L. Sun, L.P. Huang, Effects of ductile cobalt on fracture behavior of Al_2O_3–TiC ceramic, Materials Science and Engineering A 323 (2002) 17–20.
[26] Z.B. Yin, C.Z. Huang, B. Zou, Influence of cobalt additive on mechanical properties and residual stress of Al_2O_3–TiC ceramic cutting tool material, Advances in Materials Research 500 (2012) 657–661.